Moraes, M.; Moraes, J.; Tashima, M.; Akasaki, J.; Soriano Martinez, L.; Borrachero Rosado, MV.; Paya Bernabeu, JJ. (30-0). Production of bamboo leaf ash by auto-combustion for pozzolanic and sustainable use in cementitious matrices. Construction and Building Materials. 208:369-380. https://doi.org/10.1016/j.conbuildmat.2019.03.007

Production of bamboo leaf ash by auto-combustion for pozzolanic and sustainable use in cementitious matrices

M.J.B. Moraes[a], J.C.B. Moraes[b], M.M. Tashima[a], J.L. Akasaki[a], L. Soriano[c], M.V. Borrachero[c], J. Payá[c]

[a] Universidade Estadual Paulista (UNESP), Faculdade de Engenharia, Campus de Ilha Solteira, São Paulo, Brasil. Grupo de Pesquisa em Materiais Alternativos de Construção – MAC.
[b] ITA - Aeronautics Institute of Technology, São Jose dos Campos, São Paulo, Brazil
[c] ICITECH - Instituto de Ciencia y Tecnología del Hormigón, Universitat Politècnica de València, València, Spain

Abstract

In the context of world concern with the environment, this study aims to characterize an auto-combustion produced bamboo leaf ash (BLA) by its pozzolanic behaviour, reactivity and its influence in the total porosity, pore size distribution, tortuosity and mechanical behaviour of cementitious matrices. The chemical and physical characterization of the BLA was carried using X-ray fluorescence, determination of amorphous silica content, X-ray diffraction, Fourier Transform Infrared Spectrophotometry (FTIR), laser granulometry and field emission scanning electron microscopy (FESEM). The assessed BLA is a siliceous material (74.23%) with an amorphous nature due to the amorphous silica content, which represents 92.33% of the total silica. The BLA was classified as highly reactive by assessing its pH and conductivity in a saturated calcium hydroxide (CH) medium for different proportions and temperatures. Frattini analysis, the study of CH:BLA pastes (Thermogravimetric analysis and FTIR) and Portland cement (OPC) /pozzolan pastes (Thermogravimetric analysis and FESEM) are in agreement with this classification. The replacement of OPC by BLA improved the mechanical behaviour of the cementitious matrices, as well their durability. All the mortars containing BLA presented very similar compressive strength to a control mortar (100% OPC) after only 3 days of curing and at the following tested curing ages: 7, 28 and 90 days. In the mercury intrusion porosimetry analysis, the pastes with 20 and 30% BLA content presented higher tortuosity or fewer connected pores than the control paste. Thus, the auto-combustion method proved to be successful and BLA is a suitable alternative for sustainable high-performance matrices.

Keywords: bamboo leaf ash, sustainable cementitious matrices, pozzolan, auto-combustion

1. Introduction

The Stockholm Conference in 1972 was a milestone in history because it was the first time in which scientists and world leaders met to discuss and find solutions regarding environmental problems, such as air pollution. Since this event, the environment and its degradation became a rising worldwide concern. In 1987, the term sustainable development was defined and popularized by the World Commission on Environment and Development, a special commission created by the United Nations [1–2]. In 1988, the Intergovernmental Panel on Climate Change (IPCC) was created [3]. In this way, the

greenhouse effect became a worldwide preoccupation and the theme of several conferences, whose focus was to establish measures to decrease the gases which cause the greenhouse effect, carbon dioxide (CO_2) being one of the main concerns.

The world concern about both, environmental degradation and greenhouse gas emissions, highlighted the importance of research in finding new sustainable alternatives to some products, among them Portland cement (OPC). OPC is responsible for high levels of carbon dioxide emission, one ton of its production generates 0.9 tons of CO_2 [4], about 7% of the global carbon dioxide emission is due to OPC manufacture [5].

One of the research solutions found to mitigate the environmental impacts caused by OPC production is its partial replacement by pozzolans derived from anthropogenic activities. These pozzolans are byproducts and wastes which end up having no appropriated function and are often wrongly discarded, causing more environmental damage.

It is well known that pozzolans improve the mechanical behaviour and durability of cementitious matrices by acting chemically and physically. The pozzolanic chemical reaction consists of the interaction between the amorphous silica and alumina present in the material and the portlandite (the composition of which includes calcium hydroxide) derived from Portland cement hydration, forming more hydrated silicates and calcium aluminates and improving the mechanical properties of the matrix [6–8]. It is essential that those oxides present an amorphous network for the reaction to occur; thus, the reached temperature and the cooling process in pozzolan production are of extreme importance. High temperatures and long periods of thermal treating, as well as the method of heating/cooling, can lead to a crystallization of the material particles [8–10].

Related to the physical effect of pozzolans, their fine particles fill the empty spaces in the matrices, which is called the filler effect, generating a more cohesive material. The nucleation effect, also associated with the particle fineness, allows a greater hydration of the Portland cement particles, increasing the amount of hydrated products [11–13].

Most pozzolans already in widespread use in civil construction, such as pulverized fly ash and silica fume, are derived from industries [14]. Agroindustry-derived pozzolans, often associated with the food industry and biomass, are widely researched and present satisfactory results. Their use in OPC blends improves the mechanical behaviour and durability of cementitious matrices [15–28]. However, their potential is not reflected in their commercial use in civil construction, which is an unrealized opportunity since the amount of agroindustry waste is greater than the industrial ones, especially in emerging countries.

Bamboo stands out among several tree species for several reasons: it is a fast-growing plant, it has the capability to grow in degraded places, it is a natural resource with multiple purposes (from food to architecture), and it has a high sequestration capacity for carbon dioxide. Bamboo is found in many regions of the world, with a total area estimated in 31.5 million hectares worldwide, with 17.36 million hectares located in Asia [29]. Nevertheless, the bamboo cultivation generates a waste: bamboo leaves, which are burned in landfills generating bamboo leaf ash (BLA) that does not have an adequate purpose, becoming a source of pollution [30 – 31].

Nevertheless, research has been undertaken to transform this waste into a sustainable alternative for civil construction. The first researchers to study this material were Dwivedi et al. [32], and Singh et al. [33], followed by Villar-Cociña et al. [34], Frías et.al [35], Roselló et al. [36] and Villar-Cociña et al. [37]. These researches concluded that the bamboo leaf ash have good pozzolanic behaviour and high reactivity. Rodier et al. [38] conducted a study with bamboo stem ash, obtained through calcination at a controlled temperature (600 °C). The ash presented silica as the main component (68.74%) and had an amorphous nature and pozzolanic behaviour. However, these studies do not present a wide range of analysis regarding the BLA characterisation and the ash reactivity, also neither of them performed an analysis of the influence of the BLA on the durability of cementitious matrices.

As opposed to previous studies [32–37], this BLA was produced through an auto-combustion process in a furnace with no controlled temperature, a simple method like that applied in a thermoelectric plant, without consuming power. This production method yields a more realistic ash for further uses than those obtained using an electric furnace with temperature control. The BLA was characterized by its chemical composition, mineralogy, granulometric distribution and particle morphology. The reactivity of the BLA was analysed by means of different methods, such as pH and conductivity in saturated calcium hydroxide medium, the Frattini test, and the study of CH:pozzolan pastes (Thermogravimetry analysis and FTIR) and OPC/pozzolan pastes (Thermogravimetry analysis and field emission scanning electron microscopy (FESEM)). A mercury intrusion porosimetry (MIP) analysis of pastes with different OPC/BLA ratios was performed to study the influence of the addition of BLA on the total porosity and pore size distribution. The assessment of the BLA's influence on the behaviour of cementitious matrices was carried out a compressive strength analysis in mortars with partial mass replacement of OPC by BLA.

2. Materials

2.1 Materials

The BLA was produced through an auto-combustion process in a furnace with no controlled temperature, only monitored using thermocouples. For this method, an initial thermal energy is provided until the leaves start to burn by itself in the furnace, then the autocombustion process begins, differently from the electric furnace, this method does not consume power. The bamboo leaves were collected from a bamboo plantation in the surroundings of the city of Ilha Solteira, Brazil. After 15 minutes of auto-combustion, the leaves achieved a maximum burning temperature of 738 °C. The BLA obtained was then sieved (300 µm), to eliminate unburned materials, and then milled for 50 minutes.

The cement used to produce the pastes and mortars was Brazilian Portland cement type CPV ARI, this cement presents no pozzolan and is more than 95% composed of clinker. The OPC used for the pastes and mortars analysis, the Brazilian CP V ARI, presented a specific surface area of about 4800 cm^2/g (Blaine method), with 0.05% retained in the sieve of 75 µm and 0.58% retained in the sieve of 45 µm. For the Frattini test Spanish Ordinary Portland cement type CEM I 52.5R was used. The calcium hydroxide ($Ca(OH)_2$) used in the CH/BLA pastes and in the pH and conductivity analysis had more than 96%

purity. The siliceous sand for the mortars showed a specific mass of 2.58 g/cm^3 and fineness modulus of 2.12.

3. Methods

3.1 Bamboo Leaf Ash Characterization

The bamboo leaf ash was chemically characterized by XRF using an XRF Philips Magix Pro. An additional chemical analysis was performed to complement the XRF chemical characterization, the determination of the amorphous silica content. The determination of the BLA amorphous silica content was based on UNE 80225 (1993) [39] with the improvement developed and proposed by Payá et al. (2001) [40]. XRD analysis was carried out to determine the material mineralogy; the instrument used was a Shimadzu XRD - 6000, with diffractogram records in the interval of 2θ between 5° and 70°, using Cu-Ka radiation with a wavelength of 1.54056Å. An FTIR analysis was performed using a Bruker TENSOR 27 in the spectrum range of 4000–400 cm^{-1}. The influence of the milling process on the particle distribution was assessed by Laser Granulometry (Mastersizer 2000 from Malvern Instruments, working in water suspension): it was possible to determine the granulometric distribution, the main diameter (D_{med}) and the median particle diameter (D_{50}). The particle morphology of the BLA, before and after milling was determined by FESEM (ZEISS ULTRA 55).

3.2 Pozzolanic Reactivity Tests

3.2.1 Electrical Conductivity and pH measurements

The use of electrical conductivity and pH measurements is a rapid and simple method to assess pozzolan reactivity [41]. The unsaturation of the system, which means the total dissolution of the CH in solid state, causes a reduction on pH and electrical conductivity values due to the pozzolan reaction with the Ca^{+2} and OH^- dissolved ions in order to form stable and insoluble products [41].The test was performed with eight different calcium hydroxide (CH):pozzolan mass ratios (1:9; 1.5:9.5; 2:8; 2.5:7.5; 3:7; 3.5:6.5; 4:6; 4.5:5.5) and three working temperatures (40, 50 and 60 °C), using a JULABO - SW22 shaking water bath in the temperature range from 20 – 99.9 °C for temperature control and a Crison micro PH2001 pHmeter and Crison micro CM2201 electrical conductometer for the pH and electrical conductivity measurements, respectively.

The electrical conductivity results will be represented in terms of loss of conductivity (Lc (%)), calculated as proposed by Tashima et al. [41]. In this method, the pozzolan reactivity is classified into three different categories: low, medium and high. After 7 days, when the loss of loss of conductivity (Lc, in %) for a determinate CH:BLA proportion reaches a value greater than 30%, a mark is placed in the proposed template (Figure 1) for the corresponding proportion and temperature. A mark placed in Zone 3 shows that the pozzolan is highly reactive; whereas Zone 2 and Zone 1 represent medium and low reactivity, respectively.

Figure 1 - Template for classification of pozzolan reactivity (modified from Tashima et al. [41])

.

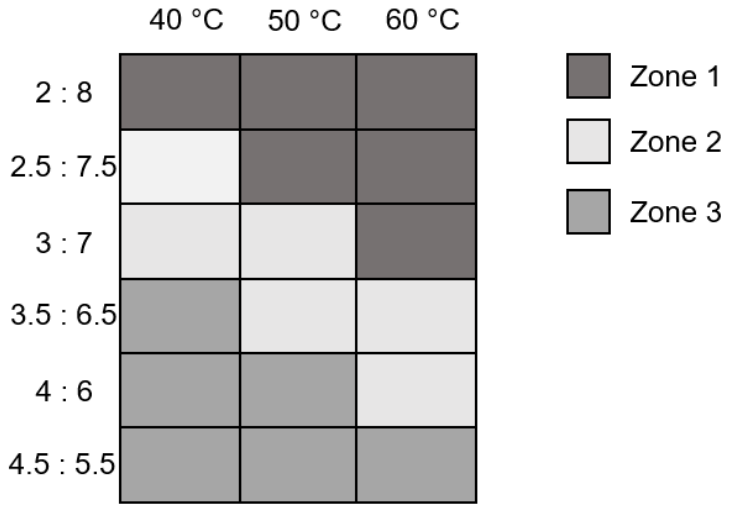

3.2.2 Frattini Test

The Frattini test analyses the pozzolanic activity and was carried out according to the procedure specified in EN 196-5 [42]. In this method, 100 mL of freshly boiled water is poured into a polyethylene container, which is sealed and placed in a thermostatic bath at 40ºC. After the thermal equilibrium is achieved, 20g of a test sample containing Portland cement CEM-I and BLA is prepared and mixed with the distilled water. The following percentages of OPC/BLA were assessed: 95/5, 90/10, 85/15, 80/20, 75/25 and 70/30. After preparation, the samples were kept for 8 and 15 days in a sealed container at 40 °C. After these periods, samples were vacuum filtered, sealed and the filtrate was cooled to room temperature. Then, the filtrate was analysed for [OH^-] by titration against diluted HCl (0.1 mol L^{-1}) with methyl orange indicator and for [Ca^{+2}] by pH adjustment to 12.50, followed by titration with 0.03 mol.L^{-1} EDTA solution using calcon indicator.

The results will be placed in a graph of [Ca^{2+}], expressed as equivalent CaO (mmol/L), versus [OH^-], in mmol/L. They will be compared to a curve which represents a saturated solution of the mentioned ions. Results below the curve of calcium oxide saturation concentration indicates removal of Ca^{2+} from the solution which is attributed to pozzolanic activity, results lying on or above the line indicates negligible pozzolanic activity.

3.2.3 Preparation and assessment of CH/BLA and OPC/BLA pastes

Pastes with three different CH:BLA proportions were prepared (3:7, 5:5 and 7:3) with a water/binder ratio of 0.8 and cured at 25 °C. For the OPC/BLA paste assessment by thermogravimetric analysis (TGA) and FESEM, a pastes were produced with no pozzolan addition and with a 15% mass replacement of OPC by BLA, both with a water/binder ratio of 0.5 and cured at 25 °C.

The CH/BLA pastes were assessed after 3, 7, 28 and 90 days of curing using FTIR (Bruker TENSOR 27 with a spectrum range of 4000 - 400 cm^{-1}) and the CH/BLA and

OPC/BLA pastes were assessed after 3, 7, 38 and 90 days of curing days by thermogravimetric analysis (TGA 850 Mettler-Toledo), in which the samples were cast in an aluminium crucible at a temperature range from 35 to 600 °C, with a heating rate of 10 °C.min^{-1}, in an N_2 atmosphere with 75 ml.min $^{-1}$ continuous gas flow and ambient pressure. The OPC/BLA pastes were analysed by FESEM (ZEISS ULTRA 55) after 28 days of curing.

The TGA enables the determination of fixed calcium hydroxide, calculated according to Payá et al. [43] for CH:BLA pastes and according to Payá et al. [44] for OPC/BLA pastes. For the OPC/BLA pastes lime consumption was also determined using Equation (1):

$$\text{Lime Consumption} = \frac{(CH_C * C) - CH_T}{100} * \frac{(1 + w/b)}{(1-C)}$$

where CH_c is the lime amount in the control paste, C is the OPC proportion in the pozzolan containing paste, CH_t is the amount of CH in the pozzolan containing paste at a determined curing age the same as the control and w/b is the water/binder ratio of the paste.

3.3 Mercury Intrusion Porosimetry (MIP)

The MIP analysis was carried out in cement pastes with water/binder ratio of 0.5 and OPC/BLA proportions of 100/0, 90/10, 80/20 and 70/30 at a curing age of 90 days at 25 ºC using an AutoPore IV 9500 porosimeter from Micrometrics Instrument Corporation with a pressure range from 13782 Pa to 227.4 MPa. The samples were evaluated at a pressure of 0.21 MPa in the low-pressure port, and 227.4 MPa in the high-pressure port.

3.4 Compressive strength of mortars

Mortars with OPC replacement by BLA in percentages of 0 (control), 5, 10, 15, 20, 25 and 30%, by mass, a water/binder ratio of 0.5 and binder:sand proportion of 1:2.5 were assessed by their compressive strength. The mortars were cast in 4 cm x 4 cm x 16 cm prismatic moulds. Samples were tested after 3, 7, 28 and 90 days of curing at 25 ºC, they were stored in full immersion in a hydrated lime saturated solution. The compressive strength was assessed following NBR 13259 [45] using an EMIC Universal Machine with a 2000 kN load limit.

4. Results

4.1 Bamboo Leaf Ash (BLA) Characterization

The chemical characterization of the BLA was obtained using an XRF and is summarized in Table 1. The ash presented a siliceous nature since it was composed mainly of silica (74.23%) and had a low quantity of Al_2O_3 (2.27%). The BLA also presented a high value of loss on ignition (LOI, 11.34%), which is attributed to the organic matter content, carbon and carbonates, present in the material. The LOI value suggested that the burning process did not completely remove the organic content of the leaves. The high value of LOI might interfere in the hydration reactions, reduce the workability of the cementitious

matrices which leads to an increase of water demand and probably a decrease of the compressive strength.

Table 1 - Chemical characterization of bamboo leaf ash (%, by mass)

SiO_2	Al_2O_3	Fe_2O_3	CaO	MgO	K_2O	SO_3	P_2O_5	Cl	TiO_2	MnO	Others	LOI
74.23	2.27	2.34	3.30	1.46	2.11	0.84	1.02	0.39	0.46	0.15	0.09	11.34

Other BLAs also derived from Brazilian bamboo [34, 35] presented silica as the main component as well, however with higher percentages: 80.4% and 78.71%, respectively, followed by CaO and K_2O. The ashes presented lower values of LOI (8.04% and 3.83%, respectively) and Al_2O_3 (1.22% and 1.01%, respectively), which shows a similar chemical composition but with differences that may be due to the type and composition of the soil and climate. Cuban ash calcinated at 700 °C [37] presented a more distinctive chemical composition, with an LOI of 3.98% and SiO_2, K_2O, CaO and SO_3 percentages of 74.7%, 5.14%, 4.48% and 4.18%, respectively.

By carrying out the procedures dictated by UNE 80225 (1993) [39] with the improvement developed by Payá et al. (2001) [40], it was possible to determine the total silica content in percentage (69.85%), which is near the XRF result (74.23%), and the total amorphous silica percentage (64.50%), which means that 92.33% of the total silica presented in BLA was in an amorphous state. This means that the potential pozzolanic reactivity of BLA is high.

The XRD analysis allows the qualitative determination of the BLA mineralogy, which means that is possible to verify if the ash presents crystalline phases, represented by characteristic peaks in the diffractogram, and if it possesses amorphousness, characterized by a deviation of the baseline between $2\theta = 15°$ and $2\theta = 35°$. The XRD pattern for BLA is shown in Figure 2; the ash presented a deviation in the baseline, which is best seen in the magnification located in the top right corner of Figure 2, which means that the BLA was amorphous in nature. However, the material also presents peaks corresponding to quartz (SiO_2, PDF Card # 0000789), the presence of this mineral is probably due to contamination of the material by soil since the leaves were collected from the ground.

The XRD results agree with the analysis of amorphous silica content since the silica presented a high content of amorphous silica which resulted in the baseline deviation and the crystalline peaks of quartz represents the remaining crystalline silica, 7.67% of the total amount of silica. The BLA found in literature showed a deviation in the baseline characteristic of an amorphous material [34,35,37], as well as quartz [37], calcite and cristobalite [35,37] and calcium sulfate [35].

Figure 2 - X-ray diffractogram pattern for the bamboo leaf ash

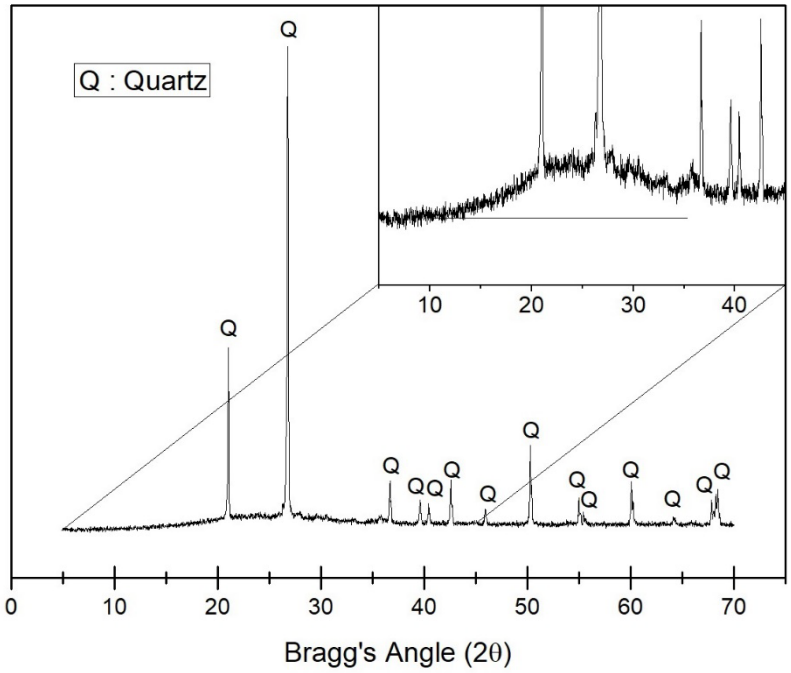

Figure 3 shows the FTIR spectrum of the BLA; it is possible to observe two bands characteristic of silicoaluminous materials, 1035 cm^{-1} and 451 cm^{-1}. The first band (1035 cm^{-1}) is associated with the vibrations from the asymmetric stretching of Si – O – Si and Si – O – Al, the second one (451 cm^{-1}) is due to the bending of Si – O – Si. The bands at 796, 777 and 694 $^{cm-1}$ indicate the symmetric bond of Si – O – Si. The FTIR spectrum confirms the siliceous nature of the material, as seen in the XRF and the determination of amorphous silica content analysis [18, 35, 46].

Figure 3 - FTIR spectrum of the bamboo leaf ash

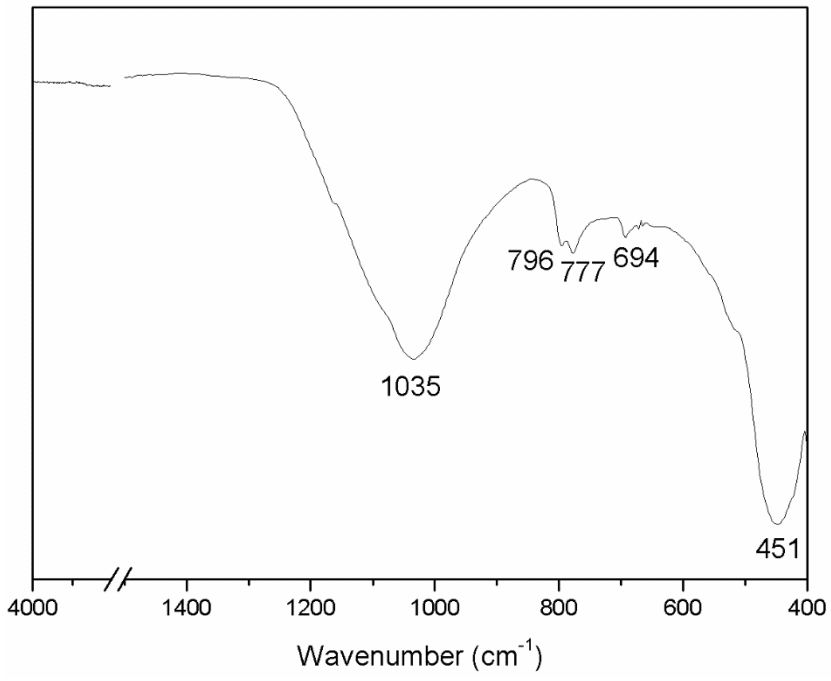

The fineness of the ash has a direct influence on its physical and chemical behaviour in the cementitious matrix; thus, the particle size distribution of the ash, after 15 kg milled for 50 minutes in a ball mill, is shown in Figure 4.

Figure 4 - Particle size distribution of the BLA, milled for 50 minutes

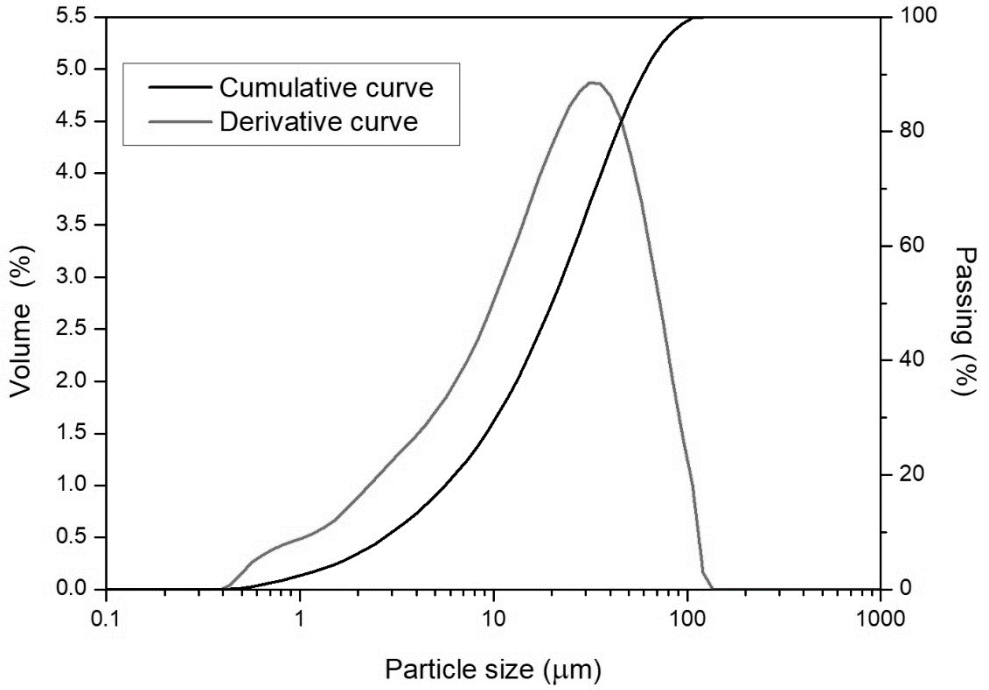

The ash presented a regular distribution: the mean particle diameter (D_{med}) was 26.1 μm, 10% of the particle volume was above 3.0 μm, 90% below 59.1 μm and the median particle diameter (D_{50}) was 20.0 μm. The influence of the milling process was also assessed by FESEM: Figure 5 shows the particle morphology of BLA before and after 50 minutes of milling. Macrostructures, such as a phytolith, can be observed in Figure 5a (spodogram or ash skeleton [36]), while in Figure 5b (milled ash) these structures are no longer present and the BLA particles showed an irregular, porous, rough form.

Figure 5 - FESEM micrographs of the BLA: a) before milling; b) after 50 minutes milling. The phytoliths are marked with arrows.

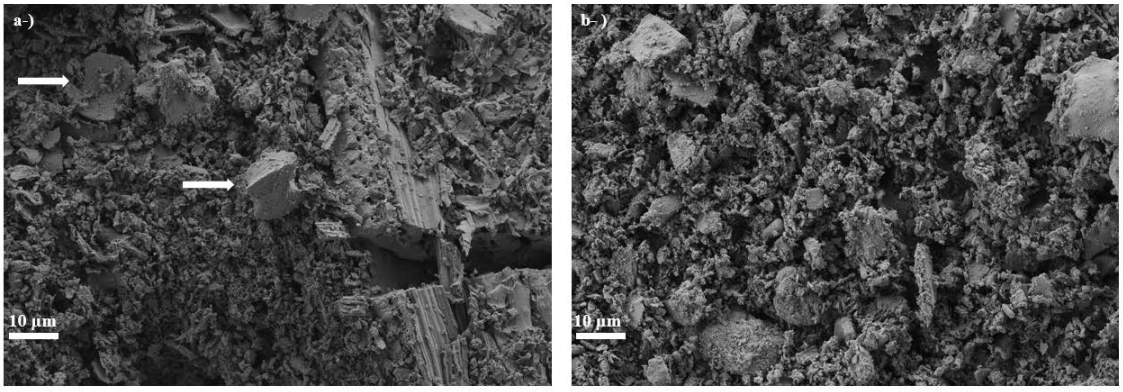

Roselló et al. [36] also observed the presence of phytoliths in BLA calcined at high temperatures and they are related to the high content of silica in the ash. Thus, the high silica content of BLA (74.23%) shown by the XRF analysis can be related to the phytoliths observed by SEM**.**

4.2 Pozzolanic Reactivity

4.2.1 Electrical Conductivity and pH in aqueous CH/BLA suspensions.

This method consists of preparing a saturated lime suspension with an excess of solid CH and mixing with the pozzolan. The consumption of the calcium hydroxide by the pozzolan would reach unsaturation with respect to CH, causing a reduction of the pH and electrical conductivity of the suspension. Eight proportions of CH:BLA were assessed at three different temperatures (40, 50 and 60 °C). As expected, the increase in the temperature caused an increase in the lime consumption for almost every sample proportion. Another expected event was that the samples with a higher percentage of CH in the proportions obtained lower values of Lc. After seven days of reaction at 60 °C, the proportions of 1:9 and 4.5:5.5 achieved an Lc of 99.08 and 31.73%, respectively; at 50 °C these proportions yielded Lc values of 98.54 and 30.87%; and at 40 °C, the values were 99.21 and 27.29%. Figure 6 shows the results of Lc as a function of time for the samples assessed at the three temperatures.

Figure 6 – Loss of electrical conductivity, Lc (%), for suspensions at: a) 60 ºC; b) 50 ºC and c) 40 ºC

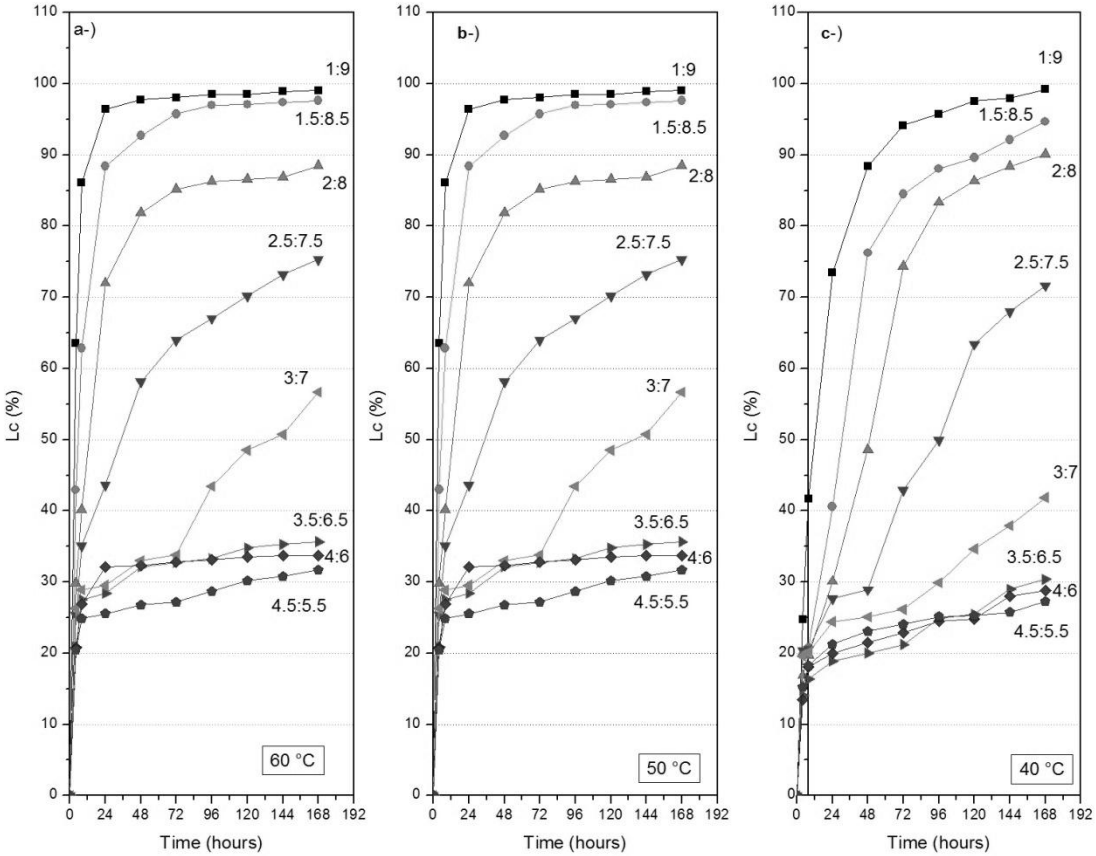

This method of analysis also enables the classification of the pozzolan as low, medium or high reactivity [41]. After seven days, when the Lc reaches a value greater than 30%, a mark is placed for the corresponding proportion and temperature in the proposed template, Figure 1. Figure 7 shows the marks placed for the proportions of CH:BLA which reached the required Lc for the three different temperatures. According to Figure 1, the BLA is placed in Zone 3, which means that the material is classified as "\high reactivity. The BLA studied was placed in the same Zone 3 which was placed an

amorphous (99% of amorphous silica) rice husk ash (RHA), a very reactive pozzolan, while a low densified silica fume (DSF-L) was placed in Zone 2, classified as medium reactive [41].

Figure 7 - Template filled for proportions at which Lc reached values higher than 30% at different temperatures

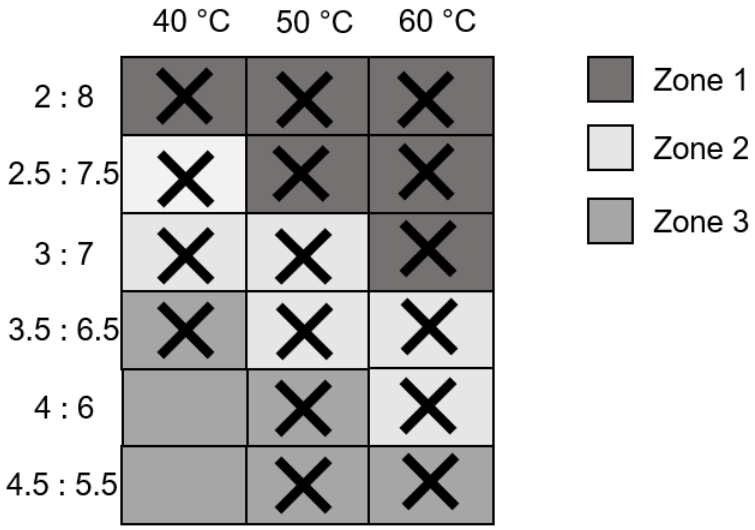

4.2.2 Frattini Test

Figure 8 shows the results obtained from Frattini Method [42]. The graph presents (for 8 days testing time), for each percentage of OPC substitution with BLA (by mass), the remaining concentration of calcium ions, expressed as calcium oxide, versus the remaining concentration of hydroxyl ions in the sample solutions kept in a sealed container at 40 °C. Those values are compared with a curve which represents a saturated solution with the mentioned ions. All the replacement percentages, except 5%, presented points under the curve after just 8 days, which indicated a high pozzolanic reactivity for the ash. In general, the increase in the replacement percentage decreases the concentration of the ions, which indicates more consumption of the ions. After 15 days, all the replacement percentages presented points below the saturated curve.

Figure 8 - Frattini tests at 8 days

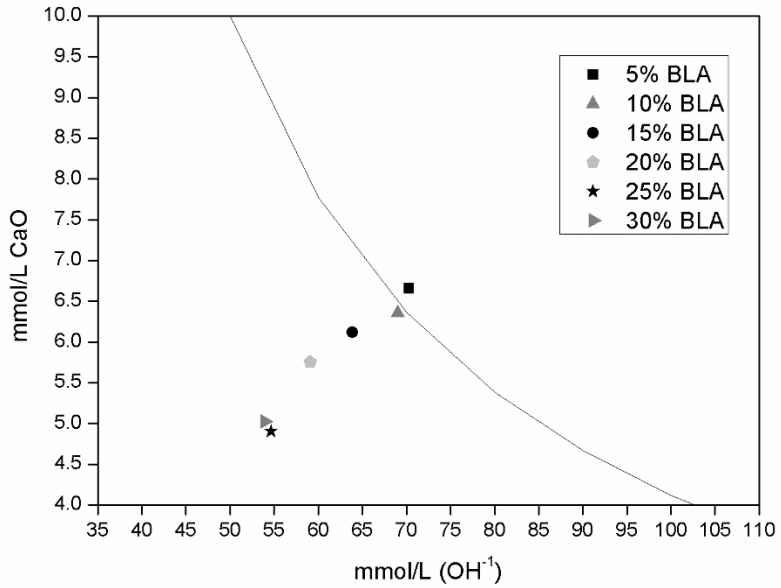

4.2.3 Analysis of calcium hydroxide/BLA pastes

Thermogravimetric and FTIR analysis were employed to analyse the performance of BLA as pozzolan in systems calcium hydroxide/BLA. Figure 9 shows the FTIR spectra for pastes prepared with CH and BLA with CH/BLA proportions of 3:7, 5:5 and 7:3 after 3, 7, 28 and 90 days of curing at 25 °C. The band at 3641 cm^{-1} present in the calcium hydroxide sample is related to its OH bonds. For pastes with a 3:7 proportion (Fig 9a), this band disappeared, which represents a complete consumption of the calcium hydroxide. As opposed to the 3:7 paste spectra, the band related to the OH bonds from CH (3641 cm^{-1}) was not entirely consumed, only decreases with curing time for samples with 5:5 (Fig 9b) and 7:3 (Fig 9c) proportions. Another confirmation of the pozzolan reaction for all proportions is the diminution in intensity of the band at 1035 cm^{-1}, associated with the vibrations of asymmetric stretching of Si – O – Si and Si – O – Al, and the appearance of a new band at 960 cm^{-1}, attributed to the calcium silicate hydrate resulting from the pozzolanic reaction [15].

The bands at 1415 cm^{-1} and 875 cm^{-1} are associated with the asymmetric stretching from the O-C-O bonds of the CO_3^{-2} groups, the carbonates probably the calcium carbonate [18]. The bands at 796 cm^{-1}, 777 cm^{-1}, 694 cm^{-1} and 451 cm^{-1} represent Si-O-Si stretching from quartz since they do not change when comparing the bands of ash and pastes. These results also confirm the presence of amorphous and crystalline silica as seen in the BLA characterization.

Figure 9 - FTIR spectra for pastes with CH:BLA ratios of: a) 3:7; b) 5:5; and c) 7:3. FTIR curves for CH and BLA are also depicted

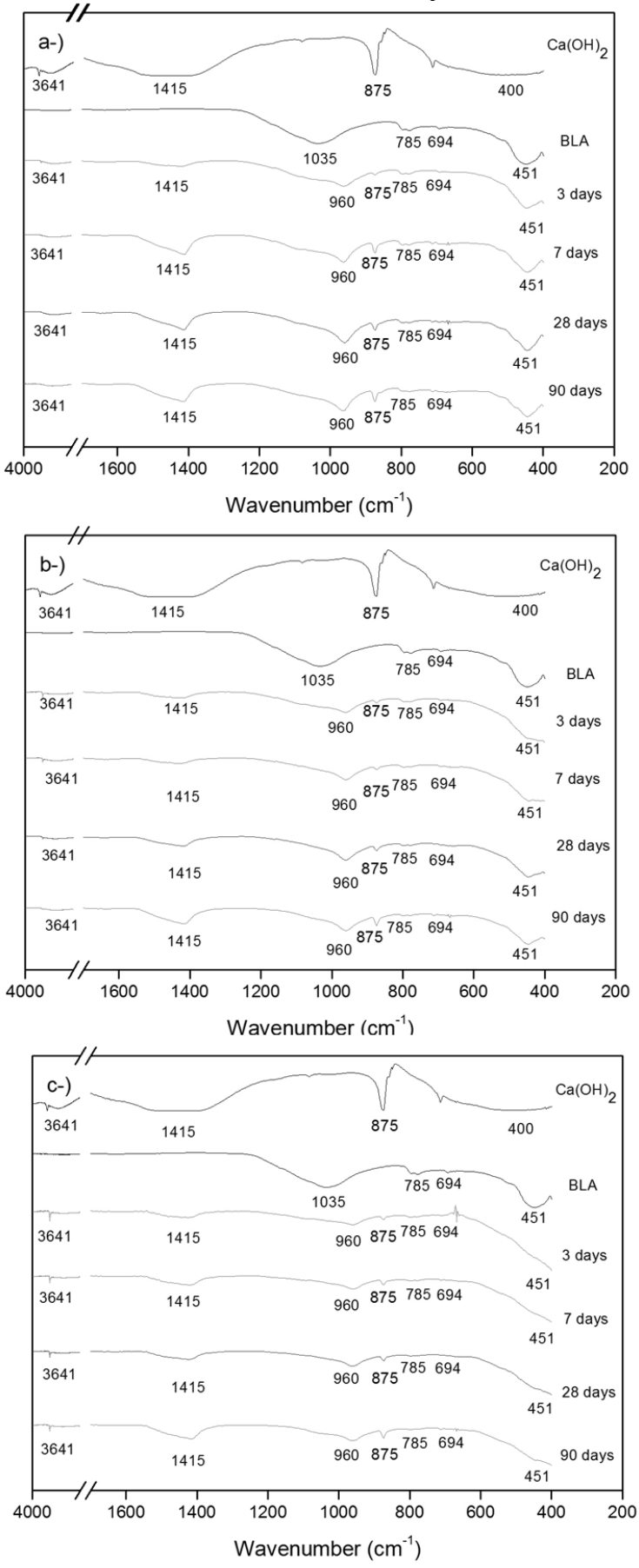

These pastes, with the same CH:BLA ratios, were also assessed by thermogravimetric analysis (TGA), Figure 10 shows the derivative thermogravimetric (DTG) curves of the pastes. There was a great consumption of the CH from 3 to 7 days for pastes with a CH:BLA ratio of 3:7, since the peak near 550 ° C decreases significantly until its complete consumption from 7 to 28 days, making a 90 days analysis unnecessary. The peaks related to the hydrated products for this proportion increased with curing age; for early ages the peaks concentrated near 120 – 130 °C, which is attributed to the dehydration of the C-S-H gel. After 7 days of curing, the gels spread through a 120 – 250 °C temperature range, which is characteristic of the dehydration of C – S – H, C – A – S – H and C – A – H gels [43].

The DTG curves for pastes with a 5:5 proportion show that there was no total consumption of calcium hydroxide since peaks close to 550 °C remained, but the intensity of the peak decreased as the curing age increased. These DTG curves also presented peaks related to the formation of hydrated calcium silicates and calcium aluminates. At early curing ages, the peaks are also concentrated near the temperatures associated with the dehydration of the C-S-H gel. After 28 days of curing, the gels rearranged and presented dehydration peaks with a range of 120 – 250 °C.

Due to the high amount of calcium hydroxide compared to pozzolan, the pastes with a CH:BLA ratio of 7:3 presented large peaks close to 550 °C for all curing ages tested. Peaks near 120 – 130 °C and 215 °C are found, indicating the formation of calcium silicate and calcium aluminate hydrated products and their rearranging over the curing ages.

Figure 10 - DTG curves for pastes of CH/BLA ratio of a) 3:7; b) 5:5; and c) 7:3

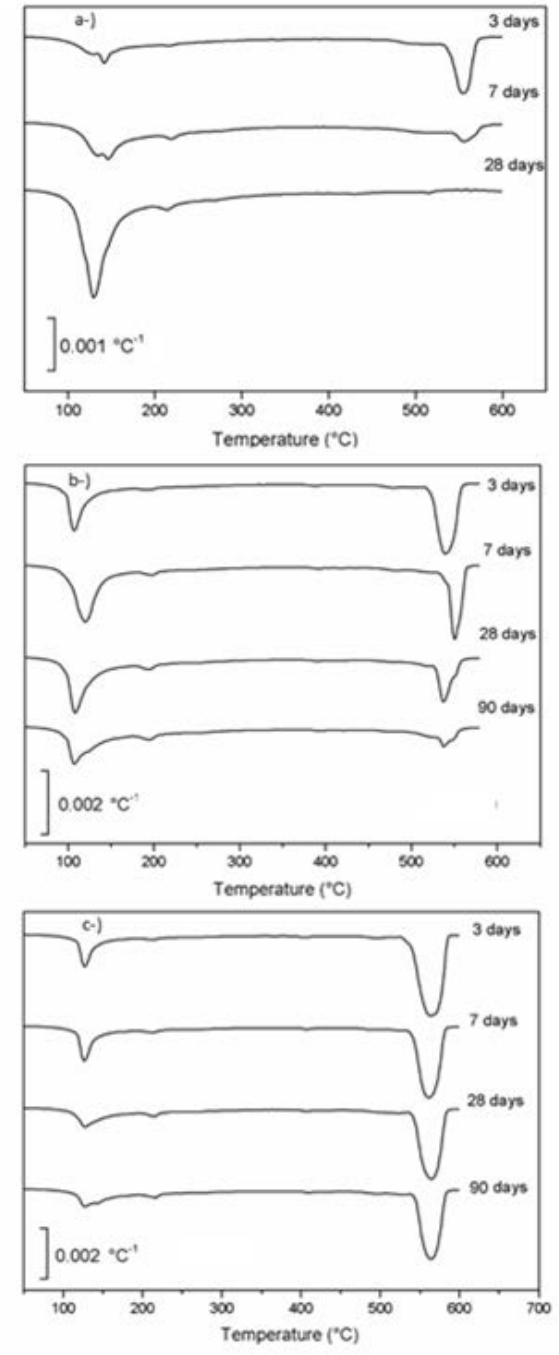

The pastes assessed by TGA underwent two dehydration processes, one during the dehydration of the pozzolan reaction resulting products (P_{PZ}) and the other during the dehydration of the unconsumed lime (P_{CH}), which allows the determination of the amount of lime fixation [43]. Table 2 shows these values as percentages.

Table 2 - Mass loss (%) relative to the dehydration of the pozzolanic reaction products (P_{PZ}), the dehydration of the unconsumed lime (P_{CH}) and the lime fixation for the CH/BLA pastes

CH:BLA ratio	Curing time (days)	P_{PZ} (%)	P_{CH} (%)	Lime fixation (%)
3 : 7	3	5.25	2.76	62.14
	7	8.88	0.68	90.70
	28	13.33	0.00	100.00
5 : 5	3	8.79	5.12	57.90
	7	11.05	3.98	67.28
	28	11.51	2.78	77.18
	90	10.76	1.74	85.70
7 : 3	3	7.13	10.11	40.62
	7	7.97	7.74	54.54
	28	8.35	7.70	54.78
	90	8.73	7.04	58.64

As seen in The FTIR analysis for pastes with a 3:7 proportion, a high consumption of the CH in early ages occurred until its complete fixation after 28 days of curing, which consequently causes an increase in the percentages of hydrated products over the curing ages, confirming once more the fast pozzolan reaction. Pastes with the same proportion of lime and metakaolin(this pozzolan is considered a high reactive pozzolan) [43], presented similar, however lower, lime fixation percentages than the lime/BLA pastes from this study. The pastes reached the values of 58.20% and 87.53%, after 3 and 7 days of curing, respectively, and a complete lime fixation (100%) between 7 and 28 days of curing. Sugar Cane Straw Ash, also a high reactive agroindustry-derived pozzolan [15], achieved a complete lime fixation (100%) after 3 days of curing, for pastes with the same CH:pozzolan ratio.

In pastes with the same amount of lime and BLA (5:5), the ash consumed more than 50% of the calcium hydroxide in only 3 days, as was also shown by the FTIR due to the large decrease of 3641 cm^{-1} for CH at three days. As seen in the FTIR, the pozzolanic reaction occurs at early ages and the formation of hydrated products increased with curing time, except for the age of 90 days, was probably due to the rearrangement of the hydrated products, as seen in the DTG curves, or a slightly carbonation, as seen in the FTIR results. The lime fixation increased from 57.90% at 3 days of curing to 85.31% at 90 days, showing that the pozzolanic reaction was fast and the reactivity was maintained during the testing period due to the presence of CH in the medium. However, for the 7:3 system, the lime fixation was very high after 3 days (40.62%), but it only increased slightly from 7 days (54.54%) to 90 days (58.64%) despite the excess of CH; this behaviour suggests that the main part of amorphous silica in BLA reacted in the first stage of the curing period.

4.2.4 Analysis of OPC/BLA pastes

The pastes with OPC/BLA ratio of 100/0 and 85/15 were assessed at 28 days of curing using an FESEM and at 3, 7, 28 and 90 days of curing using a TGA.

The DTG curves resulting from the TG analysis of the OPC/BLA pastes are shown in Figure 11. All the samples presented peaks between 120 °C and 150 °C, which means that ettringite (AFt) and C-S-H hydration products have been formed, and peaks near 220 °C, indicating the formation of hydrated products derived of aluminate (C-A-H, AFm). After 90 days of curing, the peak distribution attributed to the hydrated products changed, which may indicate a small rearrangement of the gels.

Figure 11 - DTG curves for OPC/BLA pastes

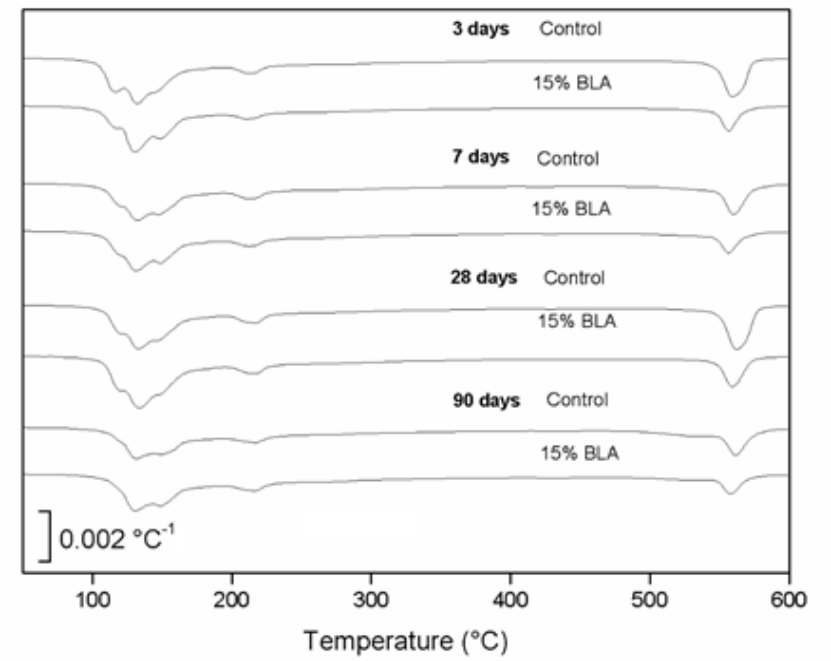

Table 3 shows the mass loss attributed to the dehydration of the products derived from the OPC hydration and the pozzolanic reaction ($P_{OPC + PZ}$), the dehydration of portlandite (P_{CH}, which was produced by OPC hydration), lime fixation [44] and lime consumption for the BLA containing pastes.

After 3 curing days, the control paste presented a higher amount of hydrated products, but at 7 days the paste with BLA exceeded the control paste and maintained a higher amount of hydrated product formation up to 90 days. The decrease of the mass loss percentage in the hydrated gels at 90 days may be due to the rearrangement of the hydrated products, as seen in Figure 11, and also to a slight carbonation of the hydrated products. P_{CH} values are lower for BLA containing samples at all curing ages, which may result from two factors: due to the pozzolanic reaction (pozzolanic contribution) and to the decrease in the amount of cement (dilution contribution), which causes a lower production of portlandite. The lime fixation and the lime consumption values indicated a high reactivity of the BLA, even for short curing ages.

Table 3 - Mass loss (%) relative to the dehydration of the OPC and pozzolanic reaction products ($P_{OPC + PZ}$), the dehydration of portlandite (P_{CH}), lime fixation and lime consumption for the OPC/BLA paste for each curing time tested

Curing time	$P_{OPC + PZ}$ (%)		P_{CH} (%)		Lime fixation	Lime Consumption*
(days)	Control	15% BLA	Control	15% BLA	(%)	
3	15.75	14.67	2.91	1.59	35.70	0.36
7	14.87	15.02	2.54	1.58	26.82	0.24
28	17.43	18.04	3.37	1.95	31.92	0.38
90	14.90	15.56	2.65	1.66	32.95	0.24

*g of fixed $Ca(OH)_2$ / g of BLA

Figure 12 shows the FESEM image for OPC/BLA ratio of 100/0 at 28 curing days. Note the amorphous gel and the presence of ettringite, which has the typical needle-like morphology.

Figure 12 - FESEM image of the control OPC paste at 28 curing days

Figure 13 shows the FESEM image of the paste with 15% OPC replacement by BLA. The image also shows the amorphous gel of the hydrated products and part of a portlandite that was not totally consumed by the pozzolanic reaction. This analysis confirms the incomplete lime fixation by BLA.

Figure 13 - FESEM image of the OPC/BLA paste with 85/15 ratio at 28 curing days (the unreacted portlandite is highlighted)

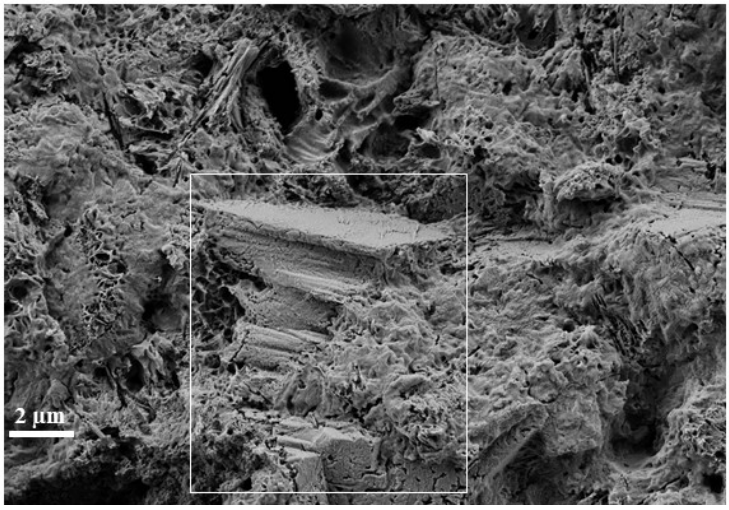

The assessment of the CH and OPC containing BLA pastes and the Frattini analysis corroborated the classification of the BLA as highly reactive pozzolan obtained by means of the pH and conductivity analysis, indicating also that the auto-combustion method of production is successful even without a controlled temperature. The other bamboo leaf ashes present in the literature also showed high reactivity [34, 35], similar to silica fume and higher than other ash-derived agro-wastes such as rice husk ash (RHA), sugar cane straw ash (SCSA) and sugarcane bagasse ash (SCBA), however they were obtained by controlled temperature methods.

4.3 Mercury Intrusion Porosimetry (MIP)

Table 4 summarizes the results of the MIP analysis and Figure 14 shows the curves of the accumulated intruded volume and the differential volume intruded for the pastes with OPC/BLA ratios of 100/0, 90/10, 80/10 and 70/10 after 90 days of curing. The results show that the paste with 20% OPC replacement by BLA presented the lowest total porosity followed by the control and the pastes with 30% BLA and 10% BLA.

The pore size distribution shown in Table 4 divided the intruded volume in each range of diameters which are classified: pores attributed to gel (< 10 nm), medium capillaries (10–50 nm), large capillaries (50 nm –1 µm) and air voids (> 1 µm).

The pastes with OPC replacement presented higher percentages of pores attributed to gels (< 10 nm), the pastes with 20% and 30% BLA presented a ratio of 21.26% and 24.61%, respectively, while the control paste achieved a ratio of 11.64%, which agrees with the reactivity study, which classified the BLA as highly reactive. The pozzolan also reduced the percentage of pores attributed to the capillarity (10 nm – 1 µm). The control paste presented a total of 84.96% capillary pores, while the paste with 20% BLA presented a total of 75.17%, about 10% of reduction.

In terms of durability, OPC replacement by BLA resulted in an improvement, since the total retained volume (Table 4) for the pastes with 20% and 30% BLA suggested less connected pores, leading to a higher tortuosity and consequently making the penetration of external agents into the matrices difficult.

In general, the MIP analyses showed how the pozzolanic reaction, the filler effect and the nucleation effect produced by the BLA improved the cementitious matrices.

Table 4 - MIP results of the OPC/BLA pastes after 90 curing days

Specimen	Total Porosity (%)	Total Retained Volume after extrusion (%)	Pore size distribution (mL of Hg/ g of paste and percentage)			
			< 10 nm	10 nm - 50 nm	50 nm - 1µm	>1µm
Control	27.64	46.78	0.0209 **(11.64%)**	0.0532 **(29.64%)**	0.0993 **(55.32%)**	0.0061 **(3.40%)**
10% BLA	29.50	44.56	0.0402 **(20.03%)**	0.0591 **(29.45%)**	0.0983 **(48.98%)**	0.0031 **(1.54%)**
20% BLA	26.14	55.70	0.0388 **(21.26%)**	0.0541 **(29.64%)**	0.0831 **(45.53%)**	0.0065 **(3.56%)**
30% BLA	28.90	55.55	0.0526 **(24.61%)**	0.0655 **(30.65%)**	0.0811 **(37.95%)**	0.0145 **(6.79%)**

Figure 14 - MIP results of the OPC/BLA pastes after 90 days of curing: a) cumulative volume intruded and b) differential volume intruded

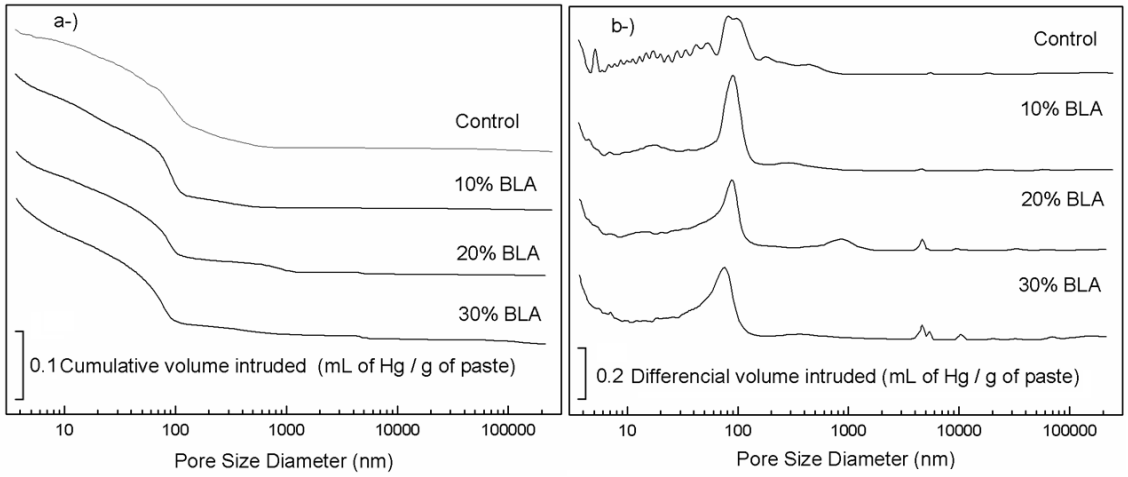

4.4 Influence of BLA on the mechanical behaviour of cementitious matrices

The influence of the BLA on the mechanical behaviour of cementitious matrices was assessed by means of a compressive strength analysis using mortar samples with OPC mass replacement by BLA, in percentages of 0 (control), 5, 10, 15, 20, 25 and 30%. Table 5 shows the values of the compressive strength results in MPa for the samples at 3, 7, 28 and 90 days of curing and the relative compressive strength of the pozzolan-containing systems regarding the control.

Initially, at early ages, almost all the BLA containing mortars presented very similar compressive strength in comparison with the control, except the mortars with replacement ratios of 25% and 30%. However, after 7 days of curing, the pozzolan-containing systems the presented very similar compressive strength in comparison with the control the for all curing ages, even with high rates of OPC replacement such as 25 and 30%, considering the standard deviation. This is a confirmation of the high reactivity of the BLA as seen in the reactivity analyses. After 28 days of curing, all the relative compressive strength is above 100%, which means that although the compressive strength is similar in

comparison with the control, the BLA slightly improved the mechanical behaviour of the matrices for later curing ages.

Table 5 - Evolution of the compressive strength of the assessed mortars after 3, 7, 28 and 90 days of curing at 25 ºC. Relative strengths (in %) for BLA containing mortars are given in parentheses.

Dosage/Curing age	*3 days*	*7 days*	*28 days*	*90 days*
	Compressive Strength (Relative Compressive Strength)			
Control	*32.75 ± 0.3*	*35.47 ± 1.6*	*43.47 ± 1.1*	*46.69 ± 1.8*
5% BLA	*32.3 ± 1.4* *(98.5%)*	*35.0 ± 1.5* *(98.6%)*	*47.3 ± 2.4* *(108.7%)*	*48.4 ± 0.3* *(103.6%)*
10% BLA	*30.1 ± 1.1* *(91.8%)*	*36.0 ± 1.0* *(101.4%)*	*46.7 ± 1.9* *(107.4%)*	*48.3 ± 1.1* *(103.4%)*
15% BLA	*33.0 ± 0.8* *(100.6%)*	*38.2 ± 1.4* *(107.6%)*	*45.6 ± 1.3* *(104.8%)*	*52.6 ± 2.0* *(112.6%)*
20% BLA	*32.2 ± 1.1* *(98.2%)*	*39.2 ± 1.7* *(110.4%)*	*46.8 ± 1.7* *(107.6%)*	*53.2 ± 2.3* *(113.9%)*
25% BLA	*29.7 ± 0.6* *(90.5%)*	*37.6 ± 1.4* *(105.9%)*	*49.2 ± 1.9* *(113.1%)*	*54.1 ± 1.9* *(115.8%)*
30% BLA	*26.7 ± 0.8*	*34.5 ± 1.2*	*43.8 ± 2.1*	*51.0 ± 2.6*

The mortars with 10% and 20% OPC mass replacement by BLA assessed by Frías et al. [35] presented a compressive strength lower, but very similar to the control after 28 and 90 days of curing. These mortars were tested for 4 x 4 x 16 cm^3 specimens, with a water/binder ratio of 0.5 and a sand/binder of 3/1.

The results of the compressive strength agree with the MIP analysis. The total porosity of the control paste and the BLA containing pastes are similar at 90 days of curing. In addition, the control paste presented a lower percentage of pores attributed to gels compared to the pastes containing BLA. In combination with the total porosity, this explains the similarity in the compressive strength results.

The improvement of the matrices by replacing OPC with BLA is even more noticeable when the compressive strength gain (SG) is calculated [47], SG is a parameter which compares the compressive strength of the control mortars, and a correction based on the replacement ratio, with the mortars with OPC replaced by BLA. The SG was calculated according to Equation (2) [47]:

$$SG = \frac{R_i - \left[R_o * \frac{w_{cem}}{w_{cem} + w_{poz}}\right]}{\left[R_o * \frac{w_{cem}}{w_{cem} + w_{poz}}\right]} * 100$$

Where R_i is the compressive strength of the pozzolan containing mortar at a determined curing age the same as the control, R_o is the compressive strength of the control mortar, w_{cem} is the OPC mass in the pozzolan containing mortar and (w_{cem} + w_{poz}) is the binder mass in the the pozzolan containing mortar.

Figure 15 shows the results of SG for the assessed mortars. The SG is positive for all the replacement ratios at all curing ages, which means the compressive strength remains the same or even improved due to the BLA reactivity even with less OPC. The SG is lower at 3 days of curing and higher after 90 days of curing for all the studied replacements, for 90 days of curing the mortar with the highest SG is the 30% BLA, with a calculated value of almost 56%; which shows not only that the BLA improves the mechanical behaviour, but also that BLA is a very sustainable alternative since a 30% OPC replacement becomes a significant OPC saving and would result in reduced environmental impacts.

Figure 15 - Strength gain (SG) of the BLA containing mortars after 3, 7, 28 and 90 curing days

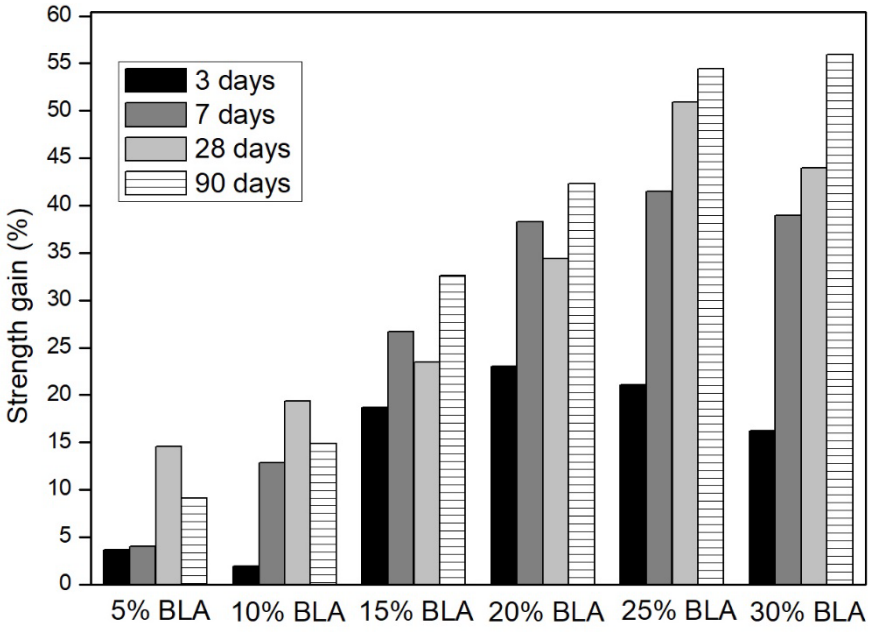

5. Conclusion

The auto-combustion produced BLA was chemically and physically characterized by means of XRF, determination of amorphous silica content, XRD, FTIR, laser granulometry and FESEM. The results showed that the assessed BLA presents a high silica content (74.23%), of which 92.33% of this oxide is amorphous silica, and obtained an 11.34% LOI, attributed to the organic matter content. The XRD corroborates the amorphous nature of the BLA by showing a baseline deviation between 2θ = 15° and 2θ = 35°, the XRD also showed the presence of quartz.

The BLA reactivity analysis the was carried out by means of pH and conductivity in aqueous $Ca(OH)_2$ medium, Frattini analysis, an FTIR study of CH:pozzolan pastes and FESEM and Thermogravimetric analysis of CH:pozzolan and OPC/pozzolan pastes. The BLA was classified as highly reactive, which means that the auto-combustion method, even though simpler (without temperature control), was successful.

The high reactivity of the BLA contributed to improved mechanical behaviour and durability of the cementitious matrices containing BLA. The pastes with 20% and 30% BLA presented less total retained volume (%) than the control paste in the MIP analysis. The mortars with OPC replacement presented very similar compressive strength after 7 curing days; the mortar with 30% BLA presented a strength gain (SG) of 56% at 90 days of curing.

BLA is a suitable and sustainable alternative for partial OPC replacement in cementitious matrices.

Acknowledgements

The authors would like to thank São Paulo Research Foundation (FAPESP), grant #2016/16403-5 and #2017/21563-4.

References

[1] G. Seyfang. Environmental mega – conferences — from Stockholm to Johannesburg and beyond, Global Environmental Change 13 (2003) 223–228. doi:10.1016/S0959-3780(03)00005-0

[2] G. Brundtland, M. Khalid, S. Agnelli, S. A. Al-Athel, B. Chidzero, L.M. Fadika, et al. Our common future: The World Commission on environment and development, Oxford: Oxford University Press 1987.

[3] Intergovernmental Panel on Climate Change - IPCC. Principles governing IPCC work. Approved at the Fourteenth Session. updated at the Thirty-Seventh session, 2013.

[4] G. Habert, C. Billard, P. Rossi, C. Chen, N. Roussel. Cement production technology improvement compared to factor 4 objectives, Cement and Concrete Research 40 (2010) 820–826. doi:10.1016/j.cemconres.2009.09.031

[5] International Energy Agency – IAE; Cement Sustainability Initiative – CSI. Technology Roadmap - Low-Carbon Transition in the Cement Industry, 2018.

[6] E. Aprianti, P. Shafigh, S. Bahri, J. N. Farahani. Supplementary cementitious materials origin from agricultural wastes – A review, Construction and Building Materials 74 (2015) 176–187. https://doi.org/10.1016/j.conbuildmat.2014.10.010

[7] Y. Senhadji, G. Escadeillas, M. Mouli, H. Khelafi, Benosman. Influence of natural pozzolan, silica fume and limestone fine on strength, acid resistance and microstructure of mortar, Powder Technology 254 (2014) 314–323. http://dx.doi.org/10.1016/j.powtec.2014.01.046

[8] F. Massazza. Pozzolana and Pozzolanic Cements. In: HEWLETT, P. C. Lea's chemistry of cement and concrete 4. ed. London: Elsevier 1998. ISBN: 978-0-7506-6256-7

[9] M. Frías. E, Villar-Cociña, H. Savastano Jr. Brazilian sugar cane bagasse ashes from the cogeneration industry as active pozzolans for cement manufacture, Cement and Concrete Composites 33 (2011) 490–496. https://doi.org/10.1016/j.cemconcomp.2011.02.003

[10] M. Frías, O. Rodríguez, M. I. S. Rojas, E. Villar-Cociña, M. S. Rodrigues, H. Savastano Jr. Advances on the development of ternary cements elaborated with biomass ashes coming from different activation process, Construction and Building Materials 136 (2017) 71–80. https://doi.org/10.1016/j.conbuildmat.2017.01.018
[11] E. Arif, M. W. Clark, N. R. Lake. Sugar cane bagasse ash from a high-efficiency co-generation boiler as filler in concrete, Construction and Building Materials 151 (2017) 692–703. https://doi.org/10.1016/j.conbuildmat.2016.10.091
[12] A. Choudhary, V. Shah, S. Bishnoi. Effect of low cost fillers on cement hydration, Construction and Building Materials 124 (2016) 533–543. http://dx.doi.org/10.1016/j.conbuildmat.2016.07.088
[13] P. Lawrence, M. Cyr, R. Ringot. Mineral admixtures in mortars — effect of inert materials on short-term hydration, Cement and Concrete Research 33 (2003) 1939–1947. doi:10.1016/S0008-8846(03)00183-2
[14] J. M. Paris, J. G. Roessler, C. C. Ferraro, H. D. DeFord, T. G. Townsend. A review of waste products utilized as supplements to Portland cement in concrete, Journal of Cleaner Production 121 (2016) 1–18. https://doi.org/10.1016/j.jclepro.2016.02.013
[15] J. C. B. Moraes, J.L. Akasaki, J. L. P. Melges, J. Monzó, M. V. Borrachero, L. Soriano, J. Payá, M. M. Tashima. Assessment of sugar cane straw ash (SCSA) as pozzolanic material in blended Portland cement: Microstructural characterization of pastes and mechanical strength of mortars, Construction and Building Materials 94 (2015) 670–677. http://dx.doi.org/10.1016/j.conbuildmat.2015.07.108
[16] R. C. Kanning, K. F. Portella, M. O. G. P. Braganca, M. M. Bonato, J. C. M. Santos. Banana leaves ashes as pozzolan for concrete and mortar of Portland cement, Construction and Building Materials 54 (2014) 460–465. http://dx.doi.org/10.1016/j.conbuildmat.2013.12.030
[17] G. C. Cordeiro, R. D. Toledo Filho, L. M. Tavares, E. M. R. Fairbairn. Experimental characterization of binary and ternary blended-cement concretes containing ultrafine residual rice husk and sugar cane bagasse ashes, Construction and Building Materials 29. (2012) 641–646. doi:10.1016/j.conbuildmat.2011.08.095
[18] J. Roselló, L. Soriano, M. P. Santamarina, J. L. Akasaki, J. Monzó, J. Payá. Rice straw ash: A potential pozzolanic supplementary material for cementing systems, Industrial Crops and Products 103 (2017) 39–50. http://dx.doi.org/10.1016/j.indcrop.2017.03.030
[19] M. M. Hossain, M. R. Karim, M. Hasan, M. K. Hossain, M. F. M. Zain. Durability of mortar and concrete made up of pozzolans as a partial replacement of cement: A review, Construction and Building Materials 116 (2016) 128–140. https://doi.org/10.1016/j.conbuildmat.2016.04.147
[20] H. Huang, X. Gao, H. Wang, H. Ye. Influence of rice husk ash on strength and permeability of ultra-high performance concrete, Construction and Building Materials 149 (2017) 621–628. https://doi.org/10.1016/j.conbuildmat.2017.05.155
[21] F. Christopher, A. Bolatito, S. Ahmed. Structure and properties of mortar and concrete with rice husk ash as partial replacement of ordinary Portland cement – A review, International Journal of Sustainable Built Environment 6 (2017) 675–692. https://doi.org/10.1016/j.ijsbe.2017.07.004
[22] M. Z. Al-mulali, H. Awang, H. P. A. Khalil, Z. S. Aljoumaily. The incorporation of oil palm ash in concrete as a means of recycling: A review, Cement and Concrete Composites. 55 (2015) 129–138. http://dx.doi.org/10.1016/j.cemconcomp.2014.09.007
[23] A. Bahurudeen, D. Kanraj, V. G. Dev, M. Santhanam. Performance evaluation of sugarcane bagasse ash blended cement in concrete, Cement and Concrete Composites 59 (2015) 77–88. https://doi.org/10.1016/j.cemconcomp.2015.03.004

[24] A. Rerkpiboon, W. Tangchirapat, C. Jaturapitakkul. Strength, chloride resistance, and expansion of concretes containing ground bagasse ash, Construction and Building Materials 101 (2015) 983–989. http://dx.doi.org/10.1016/j.conbuildmat.2015.10.140
[25] J. C. Arenas-Piedrahita, P. Montes-García, J. M. Mendoza-Rangel, H. Z. López Calvo, P. L. Valdez-Tamez, J. Martínez-Reyes. Mechanical and durability properties of mortars prepared with untreated sugarcane bagasse ash and untreated fly ash, Construction and Building Materials 105 (2016) 69–81. https://doi.org/10.1016/j.conbuildmat.2015.12.047
[26] G. C. Cordeiro, C. P. Sales. Pozzolanic activity of elephant grass ash and its influence on the mechanical properties of concrete, Cement and Concrete Composites 55 (2015) 331–336. http://dx.doi.org/10.1016/j.cemconcomp.2014.09.019
[27] A. Joshaghani, M. A. Moeini. Evaluating the effects of sugar cane bagasse ash (SCBA) and nanosilica on the mechanical and durability properties of mortar, Construction and Building Materials 152 (2017) 818–831. http://dx.doi.org/10.1016/j.conbuildmat.2017.07.041
[28] P. S. Gar, N. Suresh, V. Bindiganavile. Sugar cane bagasse ash as a pozzolanic admixture in concrete for resistance to sustained elevated temperatures, Construction and Building Materials 153 (2017) 929–936. http://dx.doi.org/10.1016/j.conbuildmat.2017.07.107
[29] Food and Agriculture Organization of the United Nations - FAO. Global Forest Resources Assessment. Main Report. 2010.
[30] J. M.O. Scurlock, D. C. Dayton, B. Hames. Bamboo: an overlooked biomass resource?, Biomass and Bioenergy 19 (2000) 229244. https://doi.org/10.1016/S0961-9534(00)00038-6
[31] M. S. I. Sohel, M. Alamgir, S. Akhter, M. Rahman. Carbon storage in a bamboo (Bambusa vulgaris) plantation in the degraded tropical forests: Implications for policy development, Land Use Policy 49 (2015) 142–151. https://doi.org/10.1016/j.landusepol.2015.07.011
[32] V. N. Dwivedi, N. P Singh, S. S. Das, N. B. Singh. A new pozzolanic material for cement industry: Bamboo leaf ash, International Journal of Physical Sciences 1 (2006) 106–111.
[33] N. B. Singh, S. S. Das, N. P. Singh, V. N. Dwivedi. Hydration of bamboo leaf ash blended Portland cement, Indian Journal of Engineering and Materials Science 14 (2007) 69–76.
[34] E. Villar-Cociña, E. V. Morales, S. V. Santos, H. Savastano Jr., M. Frías. Pozzolanic behavior of bamboo leaf ash: Characterization and determination of the kinetic parameters, Cement and Concrete Composites 33 (2011) 69–73. https://doi.org/10.1016/j.cemconcomp.2010.09.003
[35] M. Frías, H. Savastano JR., E. Villar-Cociña, S. Santos, M. I. S. Rojas. Characterization and properties of blended cement matrices containing activated bamboo leaf wastes, Cement and Concrete Composites 34 (2012) 1019–1023. https://doi.org/10.1016/j.cemconcomp.2012.05.005
[36] J. Roselló, L. Soriano, M. P. Santamarina, J. L. Akasaki, J. L. P. Melges, J. Payá. Microscopy Characterization of Silica-Rich Agrowastes to be used in Cement Binders: Bamboo and Sugarcane Leaves, Microscopy and Microanalysis 21(2015) 1314–1326. doi:10.1017/S1431927615015019
[37] E. Villar-Cociña, H. Savastano Jr., L. Rodier, M. Lefran, M. Frías. Pozzolanic Characterization of Cuban Bamboo Leaf Ash: Calcining Temperature and Kinetic

Parameters, Waste Biomass Valor 9 (2018) 691–699. https://doi.org/10.1007/s12649-016-9741-8
[38] L. Rodier, K. Bilba, C. Onésippe, M.-A. Arsène. Study of pozzolanic activity of bamboo stem ashes for use as partial replacement of cement, Materials and Structures (2017) 50–87. 10.1617/s11527-016-0958-6
[39] UNE 80225:1993 Métodos de ensayo de cementos. Análisis Químico. Determinación del dióxido de silicio (SiO_2) reactivo en los cementos, en las puzolanas y en las cenizas volantes.
[40] J. Payá, J. Monzó, M.V. Borrachero, A. Mellado, L. M. Ordoñez. Determination of amorphous silica in rice husk ash by a rapid analytical method, Cement and Concrete Research 31 (2001) 227–231. https://doi.org/10.1016/S0008-8846(00)00466-X
[41] M. M. Tashima, L. Soriano, J. Monzó, M. V. Borrachero, J. L. Akasaki, J. Payá. New method to assess the pozzolanic reactivity of mineral admixtures by means of pH and electrical conductivity measurements in lime: pozzolan suspensions, Materiales de Construcción 64 (2014) 1–12. http://dx.doi.org/10.3989/mc.2014.00914
[42] UNE – EN 196-5:2011 Métodos de ensayo de cementos: Parte 5: Ensayo de pozolanicidad para los cementos puzolánicos.
[43] J. Payá, J. Monzó, M.V. Borrachero, S. Velázquez, M. Bonilla. Determination of the pozzolanic activity of fluid catalytic cracking residue. Thermogravimetric analysis studies on FC3R–lime pastes, Cement and Concrete Research 33 (2003) 1085–1091. doi:10.1016/S0008-8846(03)00014-0
[44] J. Payá, J. Monzó, M.V. Borrachero, S. Velázquez. Evaluation of the pozzolanic activity of fluid catalytic cracking catalyst residue (FC3R). Thermogravimetric analysis studies on FC3R-Portland cement pastes, Cement and Concrete Research 33 (2003) 603–609. https://doi.org/10.1016/S0008-8846(02)01026-8
[45] NBR 13279:2005 Argamassa para assentamento e revestimento de paredes e tetos. Determinacao da resistencia a flexao e a compressao.
[46] A. Fauzi, M. F. Nuruddina, A. B. Malkawia, M. M. Al Bakri Abdullahb. Study of Fly Ash Characterization as a Cementitious Material, Procedia Engineering 148 (2016) 487–493. https://doi.org/10.1016/j.proeng.2016.06.535
[47] J. Payá, J. Monzó, M.V. Borrachero. Physical, chemical and mechanical properties of fluid catalytic cracking catalyst residue (FC3R) blended cements, Cement and Concrete Research 31 (2001) 57–61. https://doi.org/10.1016/S0008-8846(00)00432-4